Earth and Planetary Science Letters 291 (2010) 182–188

Contents lists available at ScienceDirect

Earth and Planetary Science Letters

journal homepage: www.elsevier.com/locate/epsl

A new 3D numerical model of cosmogenic nuclide ^{10}Be production in the atmosphere

Gennady A. Kovaltsov [a], Ilya G. Usoskin [b,*]

[a] Ioffe Physical–Technical Institute, St. Petersburg, Russia
[b] Sodankylä Geophysical Observatory (Oulu unit), University of Oulu, Finland

ARTICLE INFO

Article history:
Received 30 September 2009
Received in revised form 5 January 2010
Accepted 6 January 2010
Available online 1 February 2010

Editor: R.W. Carlson

Keywords:
cosmic rays
Earth's atmosphere
cosmogenic isotopes

ABSTRACT

A new quantitative model of production of the cosmogenic isotope ^{10}Be by cosmic rays in the Earth's atmosphere is presented. The CRAC:10Be (Cosmic Ray induced Atmospheric Cascade for ^{10}Be) model is based on a full numerical Monte-Carlo simulation of the nucleonic–electromagnetic–muon cascade induced by cosmic rays in the atmosphere and is able to compute the isotope's production rate at any given 3D location (geographical and altitude) and time, for all possible parameters including solar energetic particle events. The model was tested against the results of direct measurements of the ^{10}Be production in a number of dedicated experiments to confirm its quantitative correctness. A set of tabulated values for the yield function is provided along with a detailed numerical recipe forming a "do-it-yourself" kit, which allows anyone interested to apply the model for any given conditions. This provides a useful tool for applying the cosmogenic isotope method in direct integration with other models, e.g., dynamical atmospheric transport.

1. Introduction

The Earth is continuously bombarded from space by energetic particles of cosmic rays, which produce nucleonic–electromagnetic–muon cascade in the Earth's atmosphere. As a byproduct of this process, various isotopes are locally produced, which are otherwise not expected to be naturally present in the Earth's environment. They are collectively called the cosmogenic isotopes. Cosmogenic isotopes, produced mainly by cosmic rays, provide a useful tool to be applicable in different studies, just to be mentioned a few, reconstructions of solar variability and terrestrial climate in the past (e.g., Raisbeck et al., 1979; Bard et al., 1997; Beer, 2000), paleomagnetic studies (Raisbeck et al., 2006), dating (Siame et al., 2004), tracing the atmospheric air dynamics (Raisbeck et al., 1981; Lal, 2007; Usoskin et al., 2009b), etc. One of the most important cosmogenic isotopes is ^{10}Be, which is useful for long-term studies of solar activity because of its long half-life of about 1.5 millions of years. Its concentration is usually measured in stratified ice cores allowing for independent dating.

There were different attempts to model the global beryllium cosmogenic isotope production in the Earth's atmosphere, as summarized in Table 1. First models were empirical and semi-empirical, based on some fragmentary measurements of secondary neutron fluxes in the atmosphere. A major breakthrough has occurred in the 1990s with the use of Monte-Carlo modelling of the cosmic ray propagation in the atmosphere (Masarik and Reedy, 1995; Masarik and Beer, 1999). Modern models include all known processes and are supposed to precisely model beryllium production. However, as apparent from the last line of Table 1, there is a large uncertainty in the global isotope's production as predicted by different models, up to a factor of two. As argued by us earlier (Usoskin and Kovaltsov, 2008), the uncertainty is related to the overall normalization of different models, likely to the conversion factor between cosmic ray intensity and flux units (see Chapters 1.6.2 and 1.6.3 in Grieder, 2001). Therefore, any quantitative result based on the models would be uncertain within a factor of 1.5–2. We note that most of the earlier models were estimating the average beryllium production, without a possibility to study its 3D distribution, and only a few (MB99/09 and partly WH07 from Table 1) are capable of simulating both altitude profiles and geographical patterns of the production. The present CRAC model provides, for the first time, a full 3D simulation of beryllium production including a possibility to merge with any other related program (e.g., atmospheric transport code).

Usually, studies based on ^{10}Be data use a simple assumption that the isotope is first homogenously mixed in some region of the atmosphere, and then deposited in natural archives such as polar ice (e.g., McCracken, 2004; McCracken et al., 2004; Usoskin et al., 2004). Typical assumptions were polar mixing (only regions above 60° latitude contribute, roughly corresponding to the polar vortex), global mixing (the entire atmosphere mixes up) and an intermediate model (the entire stratosphere but only polar troposphere contribute to the polar ^{10}Be precipitation). Then the deposited beryllium amount is assumed to be directly proportional to the production averaged over the corresponding region. In the framework of this method, the normalization uncertainty of the production model is not important, since an ad hoc proportionality factor is anyhow used. Recently, a new realistic approach has been developed that combines the isotope

* Corresponding author.
E-mail address: ilya.usoskin@oulu.fi (I.G. Usoskin).

0012-821X/$ – see front matter © 2010 Elsevier B.V. All rights reserved.
doi:10.1016/j.epsl.2010.01.011

Table 1
Comparison of the parameters of models for the global beryllium isotope production (in atoms cm^{-2} s^{-1}, averaged over a solar cycle) in the atmosphere: LP67 — (Lal and Peters, 1967; Lal and Suess, 1968); OB79 — (O'Brien, 1979; O'Brien et al., 1991); L88 — (Lal, 1988); MR95 — (Masarik and Reedy, 1995); MB99 — (Masarik and Beer, 1999); K00 — (Kollár et al., 2000); N00 — (Nagai et al., 2000); WH03/07 — (Webber and Higbie, 2003; Webber et al., 2007); MB09 — (Masarik and Beer, 2009); CRAC — this work (for ^{10}Be) and (Usoskin and Kovaltsov, 2008) for ^{7}Be.

Model	LP67	OB79	L88	MR95	MB99	K00	N00	WH03/07	MB09	CRAC
Method[a]	Emp	Analyt	Semi-emp	MC	MC	MC	Semi-emp	MC	MC	MC
^{7}Be	0.08	0.063	N/A	0.013	0.035	0.053	≈0.06	0.035	0.04	0.062
^{10}Be	0.045	≈0.03	≈0.04	0.02	0.018	0.032	≈0.03	0.019	0.021	0.032

[a] MC — Monte-Carlo simulations; Emp — empirical; and Analyt — analytical approximation.

production model with a direct simulation of the beryllium transport using a general circulation model (e.g., Field et al., 2006; Heikkilä et al., 2009; Pedro et al., 2006; Usoskin et al., 2009b). This approach is capable of computing the absolute isotope's deposition, in contrast to the ad hoc proportionality used earlier. This has been demonstrated in a case study (Usoskin et al., 2009b), when the concentrations of another beryllium isotope ^{7}Be actually measured in different sites around the globe in January–February 2005 has been well reproduced by a production + transport combined model. For this approach it is crucially important to resolve the problem with the normalization of production models.

In order to use a realistic combined model, the isotope production model needs to provide the output in 3D (geographical coordinates and altitude) and time. Most earlier models do not provide information on the altitudinal profiles of the isotope production. Even though some of them are capable of doing 3D modelling, this information is not available in the published version or is lacking a clear numerical recipe.

Here we present a new numerical model of ^{10}Be production in the Earth's atmosphere, called CRAC:10Be (Cosmic Ray Atmospheric Cascade for ^{10}Be), which is based on a full physical Monte-Carlo simulations (see Section 2). In order to test the quantitative validity of the model, we compare it with direct production experiments (Section 3). The model is valid in variable solar activity conditions in the entire atmosphere. It is also capable of computing the effect of solar energetic particles. We also provide a detailed numerical recipe (see Appendix) and a set of pre-calculated tables that forms a do-it-yourself kit, so that a user can compute the production rate of ^{10}Be at any location and time and possible merge it with another model (e.g., an atmospheric circulation code).

2. Modelling isotope production in the atmosphere

The isotope ^{10}Be is produced in the atmosphere mainly as a result of spallation of oxygen and nitrogen caused by energetic protons, neutrons and α-nuclei. These energetic particles can be either primary cosmic rays in the upper atmosphere or nucleonic secondaries of the cascade initiated by interactions of cosmic rays in the atmosphere. Here we present a new numerical model CRAC:10Be to compute the production of the isotope in the atmosphere under various conditions. The model includes full simulation of the atmospheric cascade using a Monte-Carlo simulation tool CORSIKA (Cosmic Ray Simulations for Kascade, version 6.617, 2007 — (Heck et al., 1998)) extended by FLUKA (version 2006.3b, 2007 — (Fassò et al., 2001)) for low energy (below 80 GeV of total energy) hadronic interactions. We used a realistic curved atmosphere, also allowing for upward moving secondary particles. The chemical composition of the atmosphere was taken as N_2, O_2 and Ar in the volume fractions of 78.1%, 21% and 0.9%, respectively. The atmosphere's density profile was modeled according to the standard U.S. atmosphere as parameterized by (Keilhauer et al., 2004). First, differential spectra of nucleonic secondaries (protons, neutrons and α-particles) of the cascade were computed by the Monte-Carlo tools in great detail for primary cosmic ray particles of prescribed type and energy. This step is identical to that of the CRAC:7Be model (Usoskin and Kovaltsov, 2008). The computed spectra were then converted with cross sections of spallation reactions producing ^{10}Be. Cross sections for spallation of oxygen and nitrogen targets by protons and neutrons have been adopted from Fig. 2 of Webber and Higbie (2003), and by α-particles — from Lange et al. (1994). The accuracy of the cross-section for such spallation reactions is typically of the order of 10% (Masarik and Reedy, 1995; Webber et al., 2003; Masarik and Beer, 2009). As the next step, we computed the yield function Y_i (units — atoms g^{-1} cm^2 sr) of the isotope production, in a way similar to that of Usoskin and Kovaltsov (2008). The yield function is defined as the number of isotope atoms produced locally in the Earth's atmosphere by primary particles of type i with the unit intensity J_i in the interplanetary space at the Earth's orbit (i.e., one primary cosmic ray nucleon with kinetic energy T falling per [sr s cm^2]. Here we assume isotropic flux of primary cosmic rays. The yield function is the main tool to compute the isotope production by cosmic rays with given energy spectrum. The tabulated yield function is presented in Tables 3 and 4 for primary cosmic protons and α-particles, respectively. Henceforth we assume the isotope production per nucleon of the incident primary particle, i.e., production by one α-particle is four times that shown here.

The production of the isotope at a given atmospheric level h (g/cm^2) and geomagnetic cutoff rigidity P_c can be computed as a sum over different species of cosmic rays of the following integrals:

$$Q(h,\phi,P_c) = \sum_i \int_{T_{c,i}}^{\infty} J_i(T,\phi) Y_i(h,T) dT, \quad (1)$$

Here ϕ is the time variable modulation potential, which depends on the level of solar magnetic activity (Gleeson and Axford, 1968; Caballero-Lopez and Moraal, 2004). J_i gives the number of nucleons (which is equal to the particle number for protons but is four times that for α-particles) expressed in units of [nucleons (cm^2 sr s GeV/nuc)$^{-1}$]. Integration of Eq. (1) is over the kinetic energy T above $T_{c,i}$, which is the kinetic energy corresponding to the local vertical geomagnetic rigidity cutoff P_c, defined as

$$T_{c,i} = T_r \cdot \left(\sqrt{\left(\frac{eZ_i \cdot P_c}{A_i \cdot T_r} \right)^2 + 1} - 1 \right), \quad (2)$$

where T_r is the proton rest mass, and Z_i and A_i are the charge and mass numbers of the cosmic ray particle, respectively. The value of $T_{c,i}$ depends on the particle's Z_i/A_i ratio which makes, together with the weaker heliospheric modulation, cosmic rays species with $A_i > 1$ important in the isotope production (Webber and Higbie, 2003). The use of the vertical cutoff is a simplification, which may underestimate the effect in the upper equatorial atmosphere (e.g. O'Brien, 2008, 2009). However, it is a commonly used approach for cosmic ray effects in the lower atmosphere (below 20 km), where contribution of obliquely incident cosmic ray particles is small (e.g., Kudela and Bobik, 2004; Kudela and Usoskin, 2004; Smart et al., 2006).

As a reasonable parametrization of the energy spectrum of galactic cosmic rays near the Earth, we use the force field approximation (Usoskin et al., 2005), where the spectrum of i^{th} specie of cosmic rays

at the Earth's orbit, J_i, is related to an unmodulated local interstellar spectrum (LIS) of the same specie, $J_{LIS,i}$ via the modulation potential ϕ (given in GV) as:

$$J_i(T,\phi) = J_{LIS,i}(T + \Phi_i)\frac{T(T+2T_r)}{(T+\Phi_i)(T+\Phi_i+2T_r)}, \quad (3)$$

where T is the particle's kinetic energy per nucleon and $\Phi_i = (eZ_i/A_i)\phi$.

Here we adopt the shape of LIS as given by Burger et al. (2000) in the form parameterized by Usoskin et al. (2005)

$$J_{LIS,p}(T) = C_i\frac{P(T)^{-2.78}}{1 + 0.4866\ P(T)^{-2.51}}, \quad (4)$$

where $C_p = 1.9$ and $C_\alpha = 0.57$ for protons and α-particles (effectively including also heavier species), respectively. If other shape of the cosmic ray primary spectrum J_i is used, e.g., for solar energetic particle events, the corresponding production of ^{10}Be can be accordingly computed. The particle's momentum (in GeV/c/nuc) is given as

$$P(T) = \sqrt{T(T + 2\cdot T_r)}, \quad (5)$$

where T is given in GeV/nuc, and $T_r = 0.938$ GeV/nuc. Note that the exact value of ϕ depends on the assumed LIS and may vary between different studies. A conversion factors between most commonly used models of ϕ can be found in Usoskin et al. (2005). The local geomagnetic cutoff P_c depends mainly on the strength of the geomagnetic dipole component and the local geomagnetic latitude and can be straightforwardly computed for different epochs (Cooke et al., 1991), using an eccentric dipole approximation of the geomagnetic field (Webber, 1962; Fraser-Smith, 1987; Usoskin et al., 2010).

Finally, we have computed 3-dimensional (h, P_c and ϕ) matrix of the ^{10}Be production rate Q, which can be found at http://cosmicrays.oulu.fi/10Be/ or requested directly from the authors. Using this matrix one can instantly evaluate the ^{10}Be production rate, due to galactic cosmic rays, for given location (quantified as the local geomagnetic rigidity cutoff P_c), and latitude and time (or actually the heliospheric magnetic potential ϕ). In the following we discuss some peculiar features of the isotope production in the atmosphere.

As an illustration, Fig. 1 shows the global mean production rate of ^{10}Be depending on the geomagnetic dipole moment and cosmic ray modulation quantified via the modulation potential ϕ. For example, the global solar cycle averaged contemporary production (for modern geomagnetic dipole moment $M/M_0 = 1$, and moderate cosmic ray modulation $\phi = 550$ MV) is 0.032 atoms cm^{-2} s^{-1} (see Table 1).

The vertical profiles of the local isotope production are shown in Fig. 2 for different conditions. The production rate is greatly dependent on the altitude, varying by several orders of magnitude between the maximum at 10–km (which corresponds to upper troposphere–lower stratosphere) and the minimum at the sea level. The effect of geomagnetic shielding is also important, changing the production rate by a factor of 3–20 (depending on the altitude) between geomagnetic poles and equator. The range of variations due to the solar cycle ranges from 15% (sea-level at the equator) to a factor of 3 (polar upper stratosphere). It is apparent that temporal variations within a solar cycle (the difference between solid and dotted curves) is much smaller, few tens of %, than the spatial changes in the altitude (more than an order of magnitude between the ground and the production maximum) and in the latitude (a factor of 5–10). Therefore, it is crucially important to make sure that the model adequately reproduces the 3D pattern of the ^{10}Be production.

Because of the complicated transport of beryllium isotope in the atmosphere, it is important to separate its production in the troposphere, from where it can quickly precipitate, and stratosphere, where it is well mixed. The tropospheric production of ^{10}Be is nearly homogeneous, at the rate of about 0.01 atom/cm^2/s, over the globe (see Fig. 3) since the reduced production rate towards the equator due to the geomagnetic shielding is roughly compensated by the enhanced height, and hence the volume, of the troposphere at lower altitudes. The stratospheric production is more variable over the globe, leading to the inhomogeneous columnar production (i.e., production within the atmospheric column of unit area). We have calculated the mean columnar production (Fig. 4), which can be roughly compared to deposition flux of ^{10}Be isotope in the polar region (see, e.g. Beer, 2000) for the three mixing assumptions, discussed in the Introduction, namely polar, medium and global mixing models. The tropospheric contribution is about 20% for the polar mixing model and 40–45% for the medium and global models. This is shown only for illustration, since a more realistic approach includes direct simulation of the beryllium transport using a general circulation model. In order to study details of the isotope deposition, the present production model needs to be combined with a realistic air transport model.

Because of the discrepancies between different models, discussed in the Introduction, it is necessary to make sure that the model presented here agrees with observations. Such a test is performed in the subsequent section using a direct test of the model.

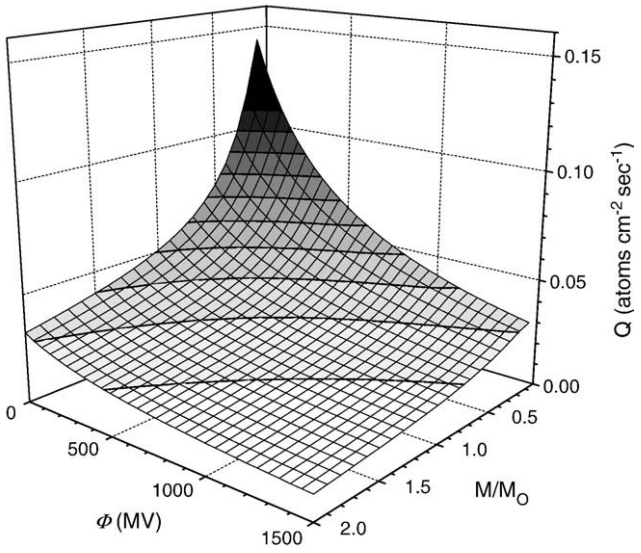

Fig. 1. Global production rate (atoms cm^{-2} s^{-1}) of ^{10}Be as function of the modulation potential ϕ and the magnetic dipole strength relative to the present one, M/M_o.

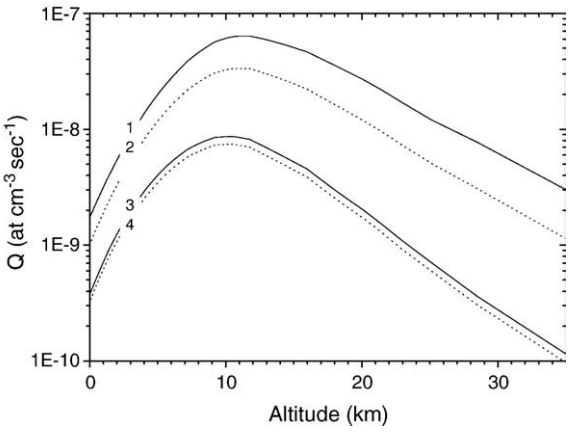

Fig. 2. Local production Q (atoms cm^{-3} s^{-1}) of ^{10}Be in the atmosphere as function of altitude. Different curves correspond to: 1 — solar minimum ($\phi = 300$ MV), polar region; 2 — solar maximum (ϕ=1000 MV), polar region; 3 — solar maximum, equator; and 4 — solar maximum, equator.

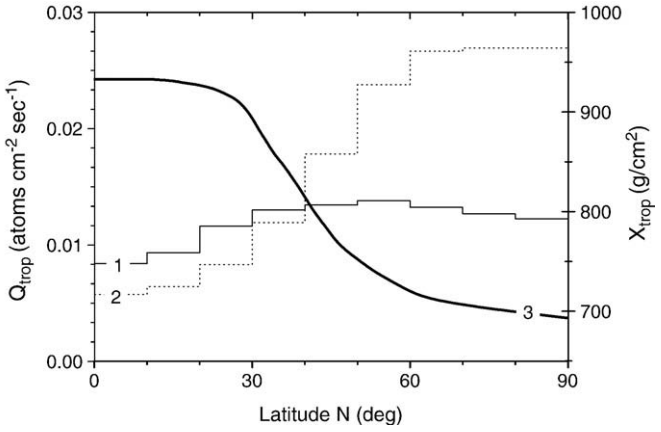

Fig. 3. Tropospheric production (atoms cm^{-2} s^{-1}) of ^{10}Be (left *Y*-axis) at moderate solar activity ($\phi = 600$ MV) and modern geomagnetic field configuration as function of Northern latitude, for the realistic (solid curve 1) and constant at $X_{trop} = 800$ g/cm^2 (dashed curve 2) tropospheric thickness. The mean realistic tropospheric thickness (right *Y*-axis), according to the World Meteorological Organization, is shown as thick curve 3.

3. Testing the model

First we notice that the core of the CRAC model — Monte-Carlo simulations of the cosmic ray induced cascade, has been tested against observations in two other applications. The code computing cosmic ray induced ionization CRAC:CRII (Usoskin and Kovaltsov, 2006) has been validated to agree with direct measurements of the atmospheric ionization rate under various conditions (Bazilevskaya et al., 2008; Usoskin et al., 2009a). This verifies the overall simulation of the cosmic-ray induced atmospheric cascade. Correctness of the nuclear production in the cascade has been further verified for another beryllium isotope, ^{7}Be, produced in similar reactions, by agreement between modelled and measured concentrations (Usoskin and Kovaltsov, 2008; Kovaltsov and Usoskin, 2009; Usoskin et al., 2009b). Now we perform a confrontation of the present CRAC:10Be model and results of direct experimental measurements of ^{10}Be production rates.

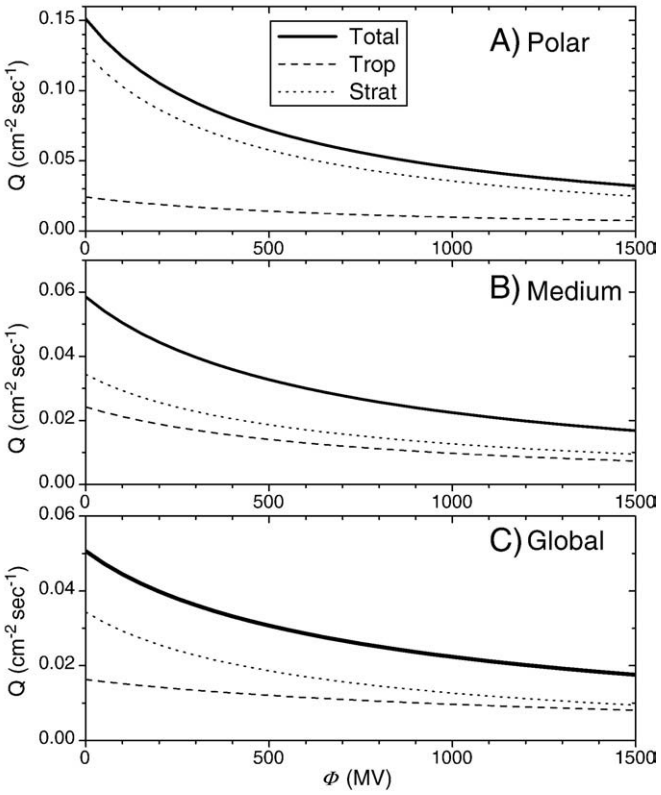

Fig. 4. Mean columnar production rate (atoms cm^{-2} s^{-1}) of ^{10}Be at the modern geomagnetic field configuration as a function of the heliospheric modulation potential ϕ for three mixing assumptions: polar, medium and global, as shown in panels A–C, respectively. In each panel, solid, dashed and dotted curves represent the total, tropospheric and stratospheric production, respectively. Notice different *Y*-axes.

In order to exclude transport effects, the production rate needs to be measured in a sealed volume. Because of the low density, it is difficult to produce a measurable amount of ^{10}Be in a gaseous air sample. As a compromise, several experiments (Nishiizumi et al., 1996; Brown et al., 2000) have been performed to measure the production rate of the isotope in a sealed water tank, where ^{10}Be isotope is produced only on oxygen. Typically, the amount of the ^{10}Be atoms produced in water exposed to cosmic ray radiation for a period of one–two years can be reliably measured using the Accelerator Mass Spectrometry technology. This provides an opportunity to directly test the production model, by means of confronting the measurements with model results obtained for the corresponding conditions and considering production of ^{10}Be only on oxygen target.

Nishiizumi et al. (1996) have performed a series of measurements of ^{10}Be in a sealed water tanks at different altitudes in two US sites (Echo Lake and La Jolla — see Table 2) during periods of moderate and high solar activity. We adopted the values of production rate, corrected for shielding, from their Table 3. Brown et al. (2000) have preformed a series of measurements of ^{10}Be in a sealed water tanks at different altitudes in French Alps (Mont Blanc, l'Aiguille du Midi and High-school — see Table 2) during a period of moderate solar activity. The production rate of ^{10}Be in water was computed as the measured concentration, corrected for shielding, background and transportation/laboratory environment (see Table 5 there) divided by the exposition period. Each measurement was then confronted with the corresponding computations by our model, using the actual parameters (altitude, geomagnetic cutoff and the modulation potential over the period of exposition) and assuming a thin target production of ^{10}Be in water, using only oxygen target cross-sections. The results are summarized in Table 2 and Fig. 5, where both measured Q_{meas} and the corresponding computed Q_{comp} values are given. One can see that the model results match nearly perfectly the measured production rates for a wide range of conditions, from the sea-level measurements in La Jolla at 1016 g/cm^2 up to the mountain altitude of 570 g/cm^2 (>4.5 km), and from moderate to high solar activity. The agreement is always within 5–6%, except ($\approx$30%) for the low-altitude high-school data, where however, much lower production rate reduces the accuracy of measurements (Brown et al., 2000) The relation between measured and modelled production rates is nearly one-to-one: $Q_{means}/Q_{comp} = 1.01 \pm 0.03$. Although beryllium production on oxygen is only about 20% of the total atmospheric production, this approach makes it possible to test the entire cascade simulation and oxygen spallation cross-sections. The nitrogen-related production is fairly similar to that on oxygen. Therefore, we believe that the overall normalization of our model is correct.

4. Concluding remarks

We have presented a new model to compute production of cosmogenic ^{10}Be isotope in the atmosphere, based on a full Monte-Carlo simulation of the cosmic ray induced nucleonic cascade in the atmosphere. The model is capable of computing 3D (altitude and geographical location) production rate of the isotope in realistic conditions. The present model is in qualitative agreement with earlier models, but deviates from some of them in the absolute values. The validity of the model, including the absolute normalization, has been verified by quantitative agreement with direct measurements of ^{10}Be production rate in several dedicated experiments.

Table 2
Production rate of ^{10}Be (10^{-}/g H_2O/s) in water, as measured by (N96 — (Nishiizumi et al., 1996)) and (B00 — (Brown et al., 2000)), as well as computed by the present model for the corresponding conditions (geomagnetic rigidity cutoff Pc, atmospheric depth h, and the mean modulation potential ϕ during the exposition period).

Measurement	Pc (GV)	h (g/cm^2)	Exposition period	ϕ (MV)	Q_{meas}	Q_{comp}
Echo Lake I [N96]	2.8	693	27/10/1988–11/09/1989	1020	2.6	2.45
Echo Lake II [N96]	2.8	693	12/09/1989–16/11/1991	1290	2.22	2.13
Echo Lake III [N96]	2.8	693	17/11/1991–12/08/1993	765	2.61	2.8
La Jolla I [N96]	5.1	1016	23/01/1989–18/10/1989	1120	0.245	0.232
La Jolla II [N96]	5.1	1016	20/10/1989–07/11/1991	1290	0.2	0.21
La Jolla III [N96]	5.1	1016	11/11/1991–05/07/1993	765	0.195	0.26
Mont Blanc I [B00]	4.8	570	05/02/1993–25/05/1994	580	4.55	4.8
Mont Blanc II [B00]	4.8	570	05/02/1993–25/05/1994	580	5.1	4.8
l'Aiguille du Midi I [B00]	4.8	644	03/02/1993–17/05/1994	580	2.8	3.0
l'Aiguille du Midi II [B00]	4.8	644	03/02/1993–17/05/1994	580	3.15	3.0
High-school [B00]	4.8	960	15/02/1993–17/06/1994	580	0.25	0.36

Table 3
Normalized yield function Y_p/π of ^{10}Be production (in atoms g^{-1} cm^2 sr) by primary cosmic protons with the energy given in GeV/nuc (Columns 2–14). Column 1 depicts the atmospheric depth h in g/cm^2.

$h\backslash T$	0.03	0.05	0.1	0.15	0.4	0.76	1.9	4.6	10.0	21.5	46.4	100
1	1.0E-10	1.4E-5	4.4E-5	5.8E-5	1.1E-4	1.5E-4	1.7E-4	1.7E-4	1.7E-4	1.7E-4	1.7E-4	1.7E-4
10	0	0	0	2.3E-4	8.5E-5	1.6E-4	1.9E-4	2.1E-4	2.4E-4	2.5E-4	2.7E-4	2.3E-4
20	0	0	0	7.4E-5	8.5E-5	1.6E-4	2.1E-4	2.3E-4	2.9E-4	3.1E-4	3.4E-4	3.0E-4
45	0	0	0	6.8E-6	7.8E-5	1.5E-4	2.3E-4	2.9E-4	3.8E-4	4.3E-4	4.9E-4	4.5E-4
100	0	0	0	9.7E-7	4.2E-5	9.5E-5	2.2E-4	3.1E-4	4.3E-4	5.3E-4	6.6E-4	6.7E-4
200	0	0	0	2.3E-7	1.5E-5	4.0E-5	1.4E-4	2.5E-4	3.8E-4	5.0E-4	6.6E-4	7.6E-4
300	0	0	0	7.0E-8	7.0E-6	2.2E-5	8.7E-5	1.7E-4	2.6E-4	3.9E-4	5.2E-4	6.8E-4
400	0	0	0	1.0E-8	2.5E-6	1.0E-5	4.3E-5	1.0E-4	1.6E-4	2.4E-4	3.7E-4	4.8E-4
500	0	0	0	0	8.0E-7	4.0E-6	2.2E-5	5.8E-5	9.6E-5	1.4E-4	2.4E-4	3.1E-4
700	0	0	0	0	2.6E-7	1.0E-6	5.1E-6	1.7E-5	2.8E-5	4.9E-5	8.4E-5	1.2E-4
850	0	0	0	0	1.8E-7	4.5E-7	1.8E-6	6.2E-6	1.1E-5	1.9E-5	3.7E-5	5.8E-5
1000	0	0	0	0	1.7E-7	2.6E-7	7.2E-7	2.4E-6	4.5E-6	6.8E-6	1.4E-5	2.3E-5

A detailed recipe (see Appendix) and a set of pre-calculated digital tables for the yield function for ^{10}Be production by cosmic rays is presented, forming a "do-it-yourself" kit. The kit makes it possible for everyone interested to compute easily production of ^{10}Be isotope at a given location, altitude and time (or the spectrum of cosmic rays). Alternatively, a set of pre-computed 3D tables of the ^{10}Be production rate can be found at http://cosmicrays.oulu.fi/10Be/ or requested directly from the authors. This provides a new opportunity in applying a cosmogenic isotope method, allowing for direct integration (i.e., without parametrization or approximation) of the present model with other models, e.g., atmospheric circulation models. This is an important step forward towards a realistic quantitative model of the dynamical beryllium production/transport/deposition in the Earth's atmosphere. The usefulness of this approach has been demonstrated using ^{7}Be isotope tracing (Usoskin et al., 2009b).

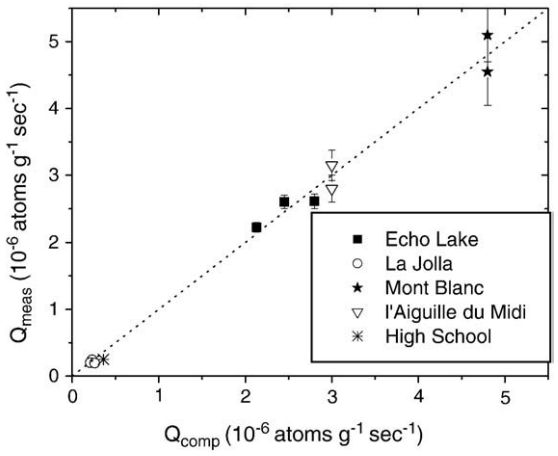

Fig. 5. Scatter plot of measured vs. computed production rates of ^{10}Be in water target (see Table 2 and text).

Acknowledgements

We acknowledge the support from the University of Oulu and the Academy of Finland. We thank the CORSIKA (http://www-ik.fzk.de/corsika/) and FLUKA (http://www.fluka.org/) teams for continuous updates and improvements of their codes. We are grateful to the Department of Physical Sciences (Astronomy Division and Space Physics group) of the University of Oulu for providing us with the computing facilities for Monte-Carlo calculations. V. Alfimov and another anonymous Reviewer are thanked for useful comments.

Appendix A. Numerical recipe of ^{10}Be production rate computations

In order to compute the ^{10}Be production rate for a given altitude h, location (geomagnetic rigidity cutoff P_c) and time (the modulation potential ϕ), one can use the following precise recipe:

1. Tabulated values of the yield function $Y(T_o,h)$ can be found in Tables 3 and 4 for protons and α-particles, respectively.
2. The value of the modulation potential ϕ can be obtained for a given period from (Usoskin et al., 2005) or from a continuously updated list at http://cosmicrays.oulu.fi/phi. The shape of the differential energy spectrum $J(T,\phi)$ is then calculated using Eq. (4) for both protons and α-particles. If another shape of the energy spectrum J is taken, e.g., for a solar energetic particle events, the corresponding isotope production can be also computed.
3. The production rate at the given location and time is finally computed using Eq. (1), where the integration bounds are different for the two species of GCR (see Eq. (2)).

Table 4
Normalized yield function Y_α/π of ^{10}Be production (in atoms g^{-1} cm^2 sr) by primary cosmic α-particles (per nucleon) with the energy given in GeV/nuc (columns 2–14). Column 1 depicts the atmospheric depth h in g/cm^2.

$h\backslash T$	0.02	0.03	0.05	0.1	0.15	0.4	0.76	1.9	4.6	10.0	21.5	46.4	100
1	1.5E-4	3.4E-4	3.2E-4	3.2E-4	3.2E-4	3.2E-4	3.1E-4	3.1E-4	3.1E-4	3.1E-4	3.1E-4	3.1E-4	3.1E-4
10	0	0	0	1.0E-7	1.2E-4	2.0E-4	2.4E-4	2.7E-4	2.9E-4	3.0E-4	3.0E-4	3.3E-4	3.5E-4
20	0	0	0	0	0	1.5E-4	2.0E-4	2.5E-4	2.9E-4	3.3E-4	3.4E-4	3.8E-4	3.8E-4
45	0	0	0	0	0	1.0E-4	1.5E-4	2.3E-4	2.9E-4	3.8E-4	4.5E-4	5.2E-4	4.3E-4
100	0	0	0	0	0	6.0E-5	1.1E-4	2.0E-4	3.0E-4	4.4E-4	5.5E-4	6.5E-4	6.0E-4
200	0	0	0	0	0	2.7E-5	6.6E-5	1.5E-4	2.6E-4	3.8E-4	5.1E-4	6.6E-4	7.6E-4
300	0	0	0	0	0	1.2E-5	3.5E-5	9.0E-5	1.7E-4	2.5E-4	4.0E-4	5.0E-4	7.0E-4
400	0	0	0	0	0	5.0E-6	1.5E-5	4.5E-5	9.9E-5	1.6E-4	2.4E-4	3.4E-4	4.7E-4
500	0	0	0	0	0	2.0E-6	7.0E-6	2.0E-5	5.5E-5	9.0E-5	1.4E-4	2.2E-4	3.0E-4
700	0	0	0	0	0	4.8E-7	1.7E-6	5.9E-6	1.7E-5	2.7E-5	4.6E-5	7.7E-5	1.2E-4
850	0	0	0	0	0	2.5E-7	7.5E-7	2.5E-6	7.0E-6	1.0E-5	2.0E-5	3.0E-5	6.0E-5
1000	0	0	0	0	0	1.6E-7	3.4E-7	9.6E-7	2.5E-6	4.3E-6	7.6E-6	1.3E-5	2.2E-5

Alternatively, one can use a set of pre-computed and tabulated production rates Q as a 3D grid of h (0–1030 g/cm^2 with the grid size of 10 g/cm^2), P_c (0–20 GV with the grid size of 0.5 GV) and ϕ (0–1500 MV with the grid size of 50 GV). The production rate then can be obtained as simply an interpolation between the grid knots. These digital tables are available at http://cosmicrays.oulu.fi/10Be/ or can be requested directly from the authors. The authors would be also glad to provide, upon requests, computation of ^{10}Be production rate for any specific location and/or time, including contribution from solar energetic particles.

References

Bard, E., Raisbeck, G.M., Yiou, F., Jouzel, J., 1997. Solar modulation of cosmogenic nuclide production over the last millennium: comparison between ^{14}C and ^{10}Be records. Earth Planet. Sci. Lett. 150, 453–462.

Bazilevskaya, G.A., Usoskin, I.G., Flückiger, E.O., Harrison, R.G., Desorgher, L., Bütikofer, R., Krainev, M.B., Makhmutov, V.S., Stozhkov, Y.I., Svirzhevskaya, A.K., Svirzhevsky, N.S., Kovaltsov, G.A., 2008. Cosmic Ray Induced Ion Production in the Atmosphere. Space Sci. Rev. 137, 149–173.

Beer, J., 2000. Long-term indirect indices of solar variability. Space Sci. Rev. 94, 53–66.

Brown, E.T., Trull, T.W., Jean-Baptiste, P., Raisbeck, G., Bourlès, D., Yiou, F., Marty, B., 2000. Determination of cosmogenic production rates of ^{10}Be, ^{3}He and ^{3}H in water. Nucl. Inst. Meth. Phys. Res. B 172, 873–883.

Burger, R.A., Potgieter, M.S., Heber, B., 2000. Rigidity dependence of cosmic ray proton latitudinal gradients measured by the Ulysses spacecraft: implications for the diffusion tensor. J. Geophys. Res. 105, 27447–27456.

Caballero-Lopez, R.A., Moraal, H., 2004. Limitations of the force field equation to describe cosmic ray modulation. J. Geophys. Res. 109, 1101.

Cooke, D.J., Humble, J.E., Shea, M.A., Smart, D.F., Lund, N., Rasmussen, I.L., Byrnak, B., Goret, P., Petrou, N., 1991. On cosmic-ray cut-off terminology. Nuovo Cimento C 14, 213–234.

Fassò, A., Ferrari, A., Ranft, J., Sala, P., 2001. Fluka: status and prospective of hadronic applications. In: A.K., et al. (Ed.), Proc. Monte Carlo 2000 Conf. Springer, Berlin, pp. 955–960.

Field, C.V., Schmidt, G.A., Koch, D., Salyk, C., 2006. Modeling production and climate-related impacts on ^{10}Be concentration in ice cores. J. Geophys. Res 111, D15107.

Fraser-Smith, A.C., 1987. Centered and eccentric geomagnetic dipoles and their poles, 1600–1985. Rev. Geophys. 25, 1–16.

Gleeson, L.J., Axford, W.I., 1968. Solar modulation of galactic cosmic rays. Astrophys. J. 154, 1011–1026.

Grieder, P.K.F., 2001. Cosmic Rays at Earth. Elsevier Science, Amsterdam.

Heck, D., Knapp, J., Capdevielle, J., Schatz, G., Thouw, T., 1998. Corsika: a Monte Carlo code to simulate extensive air showers. FZKA 6019. Forschungszentrum, Karlsruhe.

Heikkilä, U., Beer, J., Feichter, J., 2009. Meridional transport and deposition of atmospheric ^{10}Be. Atmos. Chem. Phys. 9, 515–527.

Keilhauer, B., Blümer, J., Engel, R., Klages, H.O., Risse, M., 2004. Impact of varying atmospheric profiles on extensive air shower observation: atmospheric density and primary mass reconstruction. Astroparticle Physics 22, 249–261.

Kollár, D., Leya, I., Masarik, J., Michel, R., 2000. Calculation of cosmogenic nuclide production rates in the Earth atmosphere and in terrestrial surface rocks using improved neutron cross sections. Meteorit. Planet. Sci. Suppl. 35, 90.

Kovaltsov, G.A., Usoskin, I.G., 2009. Test of production models for beryllium cosmogenic radionuclides in the Earth's atmosphere. Procs. 31st Internat. Cosmic Ray Conf. Lodz, Poland. p. ID:icrc0163.

Kudela, K., Bobik, P., 2004. Long-term variations of geomagnetic rigidity cutoffs. Solar Phys. 224, 423–431.

Kudela, K., Usoskin, I.G., 2004. On magnetospheric transmissivity of cosmic rays. Czec. J. Phys. 54, 239–254.

Lal, D., 1988. Theoretically expected variations in the terrestrial cosmic-ray production rates of isotopes. In: Cini Castagnoli, G. (Ed.), Solar–Terrestrial Relationships and the Earth Environment in the last Millennia. Soc. Italiana di Fisica, Bologna, pp. 216–233.

Lal, D., 2007. Recycling of cosmogenic nuclides after their removal from the atmosphere; special case of appreciable transport of ^{10}Be to polar regions by aeolian dust. Earth Planet. Sci. Lett. 264, 177–187.

Lal, D., Peters, B., 1967. Cosmic ray produced radioactivity on the earth. In: Sittle, K. (Ed.), Handbuch der Physik, vol. 46/2. Springer-Verlag, Berlin, pp. 551–612.

Lal, D., Suess, H., 1968. The radioactivity of the atmosphere and hydrosphere. Ann. Rev. Nuc. Sci. 18, 407–434.

Lange, H.-J., Hahn, T., Michel, R., T.S., et al., 1994. Production of residual nuclei by α-induced recations on c, n, o, mg, al and si up to 170 MeV. Appl. Radiat. Isot. 46, 93–112.

Masarik, J., Beer, J., 1999. Simulation of particle fluxes and cosmogenic nuclide production in the Earth's atmosphere. J. Geophys. Res. 104, 12099–12111.

Masarik, J., Beer, J., 2009. An updated simulation of particle fluxes and cosmogenic nuclide production in the Earth's atmosphere. J. Geophys. Res. 114, D11103.

Masarik, J., Reedy, R.C., 1995. Terrestrial cosmogenic-nuclide production systematics calculated from numerical simulations. Earth Planet. Sci. Lett. 136, 381–395.

McCracken, K.G., 2004. Geomagnetic and atmospheric effects upon the cosmogenic ^{10}Be observed in polar ice. J. Geophys. Res. 109, A04101.

McCracken, K., McDonald, F., Beer, J., Raisbeck, G., Yiou, F., 2004. A phenomenological study of the long-term cosmic ray modulation, 850–1958 AD. J. Geophys. Res. 109 (A18), 12103.

Nagai, H., Tada, W., Kobayashi, T., 2000. Production rates of ^{7}Be and ^{10}Be in the atmosphere. Nucl. Instrum. Meth. Phys. Res. B 172, 796–801.

Nishiizumi, K., Finkel, R.C., Klein, J., Kohl, C.P., 1996. Cosmogenic production of ^{7}Be and ^{10}Be in water targets. J. Geophys. Res. 101, 22225–22232.

O'Brien, K., 1979. Secular variations in the production of cosmogenic isotopes in the Earth's atmosphere. J. Geophys. Res. 84, 423–431.

O'Brien, K., 2008. Limitations of the use of the vertical cut-off to calculate cosmic-ray propagation in the Earth's atmosphere. Rad. Prot. Dosimetry 128, 259–260.

O'Brien, K., 2009. Erratum: limitations of the use of the vertical cut-off to calculate cosmic-ray propagation in the Earth's atmosphere. Rad. Prot. Dosimetry 399, 259–260.

O'Brien, K., de La Zerda Lerner, A., Shea, M., Smart, D., 1991. The production of cosmogenic isotopes in the Earth's atmosphere and their inventories. In: Sonett, C.P., Giampapa, M.S., Matthews, M.S. (Eds.), The Sun in Time. The University of Arizona, pp. 317–342.

Pedro, J., van Ommen, T., Curran, M., Morgan, V., Smith, A., McMorrow, A., 2006. Evidence for climate modulation of the ^{10}Be solar activity proxy. J. Geophys. Res. 111, D21105.

Raisbeck, G.M., Yiou, F., Fruneau, M., Loiseaux, J.M., Lieuvin, M., 1979. ^{10}Be concentration and residence time in the ocean surface layer. Earth Planet. Sci. Lett. 43, 237–240.

Raisbeck, G.M., Yiou, F., Fruneau, M., Loiseaux, J.M., Lieuvin, M., Ravel, J.C., 1981. Cosmogenic Be-10/Be-7 as a probe of atmospheric transport processes. Geophys. Res. Lett. 8, 1015–1018.

Raisbeck, G.M., Yiou, F., Cattani, O., Jouzel, J., 2006. ^{10}Be evidence for the Matuyama-Brunhes geomagnetic reversal in the EPICA Dome C ice core. Nature 444, 82–84.

Siame, L., Bellier, O., Braucher, R., Sébrier, M., Cushing, M., Bourlès, D., Hamelin, B., Baroux, E., de Voogd, B., Raisbeck, G., Yiou, F., 2004. Local erosion rates versus active tectonics: cosmic ray exposure modelling in Provence (south-east France). Earth Planet. Sci. Lett. 220, 345–364.

Smart, D.F., Shea, M.A., Tylka, A.J., Boberg, P.R., 2006. A geomagnetic cutoff rigidity interpolation tool: accuracy verification and application to space weather. Adv. Space Res. 37, 1206–1217.

Usoskin, I., Mursula, K., Solanki, S., Schüssler, M., Alanko, K., 2004. Reconstruction of solar activity for the last millennium using ^{10}Be data. Astron. Astrophys. 413, 745–751.

Usoskin, I.G., Alanko-Huotari, K., Kovaltsov, G.A., Mursula, K., 2005. Heliospheric modulation of cosmic rays: monthly reconstruction for 1951–2004. J. Geophys. Res. 110, A12108.

Usoskin, I.G., Desorgher, L., Velinov, P., Storini, M., Flückiger, E.O., Bütikofer, R., Kovaltsov, G.A., 2009a. Ionization of the Earth's atmosphere by solar and galactic cosmic rays. Acta Geophys. 57, 88–101.

Usoskin, I.G., Field, C.V., Schmidt, G.A., Leppänen, A.-P., Aldahan, A., Kovaltsov, G.A., Possnert, G., Ungar, R.K., 2009b. Short-term production and synoptic influences on atmospheric ^{7}Be concentrations. J. Geophys. Res. 114, D06108.

Usoskin, I.G., Kovaltsov, G.A., 2006. Cosmic ray induced ionization in the atmosphere: full modeling and practical applications. J. Geophys. Res. 111, D21206.

Usoskin, I.G., Kovaltsov, G.A., 2008. Production of cosmogenic ^{7}Be isotope in the atmosphere: full 3-D modeling. J. Geophys. Res. 113, D12107.

Usoskin, I.G., Mironova, I., Korte, M., Kovaltsov, G.A., 2010. Regional millennial trend in the cosmic ray induced ionization of the troposphere. J. Atmos. Solar-Terr. Phys. 72, 19.

Webber, W., 1962. Time variations of low rigidity cosmic rays during the recent sunspot cycle. In: Wilson, J., Wouthuysen, S. (Eds.), Progress in Elementary Particle and Cosmic Ray Physics, vol. 6. Amsterdam, North Holland, pp. 77–243.

Webber, W.R., Higbie, P.R., 2003. Production of cosmogenic Be nuclei in the Earth's atmosphere by cosmic rays: its dependence on solar modulation and the interstellar cosmic ray spectrum. J. Geophys. Res. 108, 1355.

Webber, W.R., Soutoul, A., Kish, J.C., Rockstroh, J.M., 2003. Updated formula for calculating partial cross sections for nuclear reactions of nuclei with $Z <= 28$ and $E > 150$ MeV nucleon^{-1} in hydrogen targets. Astrophys. J. Suppl. Ser. 144, 153–167.

Webber, W.R., Higbie, P.R., McCracken, K.G., 2007. Production of the cosmogenic isotopes ^{3}H, ^{7}Be, ^{10}Be, and ^{36}Cl in the Earth's atmosphere by solar and galactic cosmic rays. J. Geophys. Res. 112, A10106.